ASTRONOMY & ASTROPHYSICS
SUPPLEMENT SERIES

OCTOBER II **1993**, PAGE 431

Astron. Astrophys. Suppl. Ser. **101**, 431-445 (1993)

Radio galaxies of intermediate strength. II. VLA observations

M. Bondi[1,2], L. Gregorini[1,3], L. Padrielli[1] and P. Parma[1]

[1] Istituto di Radioastronomia CNR, Bologna, Italy
[2] Dipartimento di Astronomia, Universitá di Bologna, Italy
[3] Dipartimento di Fisica, Universitá di Bologna, Italy

Received January 27; accepted February 12, 1993

Abstract. — We present radio observations of 14 4C radio galaxies with intermediate radio power. The observations were carried out with the Very Large Array (A and D configuration) at 20 cm; furthermore 9 sources were also observed at 5 GHz (C configuration). From all the data we selected the most accurate and important parameters for the description of the radio structures; contour maps of the sources are given.

Key words: galaxies: elliptical — galaxies: general — radio continuum: galaxies

1. Introduction

This is the second paper concerning the study of a sample of 4C radio galaxies made with the VLA at 20 cm. The study of the radio structure of this sample is interesting because it forms the natural link between B2 and 3C radio galaxies. In fact the median radio power of the 4C sample (log P(1.4 GHz) = 25.2) corresponds to the change between edge darkened and edge brightened morphologies.

The previous paper (Gregorini et al. 1988, hereafter referred to as paper I) presented VLA B-configuration observations of all sources, for which high resolution and sensitivity data were not available.

Here we present additional observations done with the A configuration for sources where information on small scale structure was necessary and observations with the D configuration for extended sources where part of flux missed. A few objects have also been observed at 5 GHz in the C configuration.

The paper is organized as follows: the description of the sample is given in Sect. 2; the observation and data reduction are presented in Sect. 3; the results and the comments on individual sources are given in Sects. 4 and 5, respectively.

Send offprint requests to: L. Gregorini

2. Redefinition of the sample

Katgert-Merkelijn et al. (1980) made a compilation of 4C radio sources using data published until then and obtained two complete samples at 408 MHz and 178 MHz in the area $25° < \delta < 31°$, $33° < \delta < 40°$ and $|b| > 15°$.

We refer to that paper for details on the definition of the sample and identification procedure. From the catalogue we selected all sources identified with galaxies brighter than m_v = 19.5 for a total of 37 objects. We also included two other radio galaxies of the list of Katgert-Merkelijn et al. (1980) not belonging to the complete sample. All sources were observed with the WSRT at 1.4 Ghz and 5 Ghz (Katgert-Merkelijn et al. 1980); 10 sources were already observed with the VLA by others, the remaining 29 sources were observed in the B configuration at 1.4 Ghz (paper I). 9 out of these 29 sources were mapped with A configuration, while for 5 sources additional observations with the D configuration were necessary.

The final sample consists of 35 radio galaxies; in fact the VLA observations revealed a total of 2 misidentifications.

3. Observations and data reduction

We refer to Napier et al. (1983) for a description of the VLA and its modes of operations.

The observations were done: with the A array in July 1987 at the frequencies of 1465 and 1515 MHz; with the D array in January 1990 at the frequencies 1465 and 1635 MHz; with the C array in July 1989 at the frequencies of 4885 and 4835 MHz. In all the observations the bandwidth was 50 MHz. Every half hour we observed a calibration source, whose flux density was bootstrapped from that of 3C286 or 3C48.

Post-calibration reduction was done using the NRAO AIPS package running on the Convex C 201 of the Istituto di Radioastronomia del CNR (Bologna) and on the Alliant FX80 of the Kapteyn Laboratorium (Groningen). The procedure followed was identical for the different arrays.

The data were carefully checked and edited out for deviating amplitudes, after they were cleaned and restored with the task MX, using the two IF's. For the D array we only present the observations at 1465 MHz, the data of the second IF being strongly affected by interferences. Self-calibration was applied to improve the dynamical range.

A summary of the observations is presented in Table 1 for the 1.4 GHz data and in Table 2 for the 5 Ghz data, respectively. The source name, the observing time, the FWHM and the position angle of the synthesized beam and the actual noise are given for each source.

We also obtained maps combining the B array data (Paper I) with A array data or D array data. In the combined map the rms noise is in the range 0.07 to 0.17 mJy/beam for the A and B arrays and in the range 0.18 to 0.30 mJy/beam for the B and D arrays.

4. results

The new contour maps are presented from Figs. 1 to 14: Fig. a for 1.4 GHz data, and Fig. b for 5 GHz data. For 1.4 GHz data we show A array or A+B array or B+D array maps selecting those with new information with respect to Paper I.

In Table 3 we present the radio parameters at 1.4 GHz. We derived these data from the more appropriate image (i.e. compact component parameters from array A maps and global parameters, such as total flux and largest angular size, from array D or combined maps). For each source we give: -in the first line- optical position, magnitude, redshift, total radio flux, largest angular size and position angle of the whole radio structure; -in the following lines we give - radio position, flux and diameters of sub-components. For slightly resolved components these parameters are determined with a bidimensional Gaussian fit and the half maximum (FWHM) and the position angle are given. For the more extended and complex components the sizes are measured in the direction of the position angle of the source axis and perpendicular to it. When a bright hot spot is present we give the position and the flux of the radio emission peak. The flux of the lobe also contains the jet if present.

The data at 5 GHz are presented in Table 4. The meaning of the column is the same as in Table 3, except for the optical information which are not repeated.

We refer to Paper I for a more detailed description of the determinations of radio parameters.

5. Comments on individual sources

0136+39: following Paper I we consider the source at 01 36 49.87 + 39 42 59.9 as a possible background source. Its total flux at 5 GHz is 18 mJy.

0204+29: in a recent paper Meurs & Unger (1991) interpreted the complex radio structure of this source as a superposition of a background source and a Seyfert galaxy. The bright hot-spot to North-East is considered a background source without optical identification, while the Seyfert galaxy is coincident with the faint radio core. The parameters in Table 3 refer to the whole source.

0258+35A: the low resolution and the combined maps at 1.4 GHz show low brightness tails completely resolved in the previous 1.4 GHz maps and in the 5 GHz map presented here.

1547+30: the new high resolution data do not confirm the previous identification; no optical counterpart has been found within the limits of the Palomar Sky Survey. However the radio parameters and the map are presented in Table 3 and Fig. 11, respectively.

1707+34: the low brightness component is resolved in the 5 GHz map.

2249+37: the new low resolution and the combined maps show an extended halo which is completely resolved in the 5 GHz map. The second compact component present at both fequencies (core2 in Table 3 and 4) is identified with a faint galaxy probably belonging to the same cluster of the 4C radio galaxy.

Acknowledgements. Part of the work was carried out during a visit by LG to the Kapteyn Laboratorium (Groningen), organized under the exchange agreement between the Consiglio Nazionale delle Ricerche and the Nederlandse Organisatie voor wetenschappelijk onderzoek. L.G. wants to thank the warm hospitality of the Kapteyn Laboratorium.

References

Gregorini L., Padrielli L., Parma P., Gilmore G. 1988, A&AS 74, 107

Katgert-Merkelijn J., Lari C., Padrielli L. 1980, A&AS 40, 91

Meurs E.J.A., Unger S.W. 1991, A&A 252, 63

Napier P.J., Thompson A.R., Ekers R.D. 1983, Proc. IEEE 71, 1295

Table 1. Observational summary at 20 cm

B2 Name	Other Name	Obs.time min	Beam ″	Pos.Angle °	Noise mJy/beam
0136+39	4C39.04	25	48.5x44.3	55	0.19
0158+29	4C29.05	35	1.1x1.1		0.18
0204+29	4C29.06	25	47.4x44.3	57	0.35
0247+39	4C39.10	30	1.3x1.3		0.14
0258+35A	4C35.06	20	50.0x42.8	67	0.16
1130+33A	4C33.27	10	1.1x1.1		0.17
1151+38	4C38.32	10	1.4x1.3	-49	0.19
1151+29	4C29.44	10	1.1x1.1		0.18
1529+35	3C320	10	1.1x1.1		0.13
1539+34	4C34.42	10	1.1x1.1		0.10
1547+30	4C30.29	10	1.3x1.2	17	0.27
1707+34	4C34.45	20	65.6x40.6	81	0.09
2244+36	4C36.47	20	1.2x1.1	-25	0.10
2249+37	4C37.66	20	41.1x36.5	14	0.18

Table 2. Observational summary at 6 cm

B2 Name	Other Name	Obs.time min	Beam ″	Pos.Angle °	Noise mJy/beam
0136+39	4C39.04	25	4.9x4.9		0.08
0204+29	4C29.06	25	3.6x3.5	17	0.14
0258+35A	4C35.06	25	3.8x3.8		0.04
1707+34	4C34.45	25	6.1x3.0	87	0.04
2249+37	4C37.66	25	3.5x2.8	-14	0.08

Table 3. Observational data at 1.4 GHz

B2 Name	Other Name	R.A. (1950) h m s	Dec. (1950) ° ′ ″	m vis	z	S mJy	FWHM P.A. arcsec °	LAS arcsec	P.A. °
0136+39	4C39.04	01 36 33.66	39 41 52.6	19.5	0.2107	985		377	63
core		33.59	51.6			33	< 2		
E lobe						490		179×56	
W lobe						459		158×50	
0158+29	4C29.05	01 58 43.20	29 19 17.2	15.9	0.1482	1215		58	7
core		43.42	16.5			12	<0.2		
S jet						37			
N lobe						475		28×30	
S lobe						711		30×32	
N hot spot		43.66	34.0			3			
S hot spot		43.59	18 51.7			5			
0204+29	4C29.06	02 04 08.78	29 16 30.5	16.5	0.109	2310		199	62
core		08.87	30.5			21	<2		
E lobe						1420		121×42	
W lobe						887		76×44	
E hot spot		16.81	17 28.5			372			
0247+39	4C39.10	02 47 04.78	39 22 08.8	18.6		1765		162	95
core		04.76	08.2			26	<0.3		
E lobe						827		77×38	
W lobe						901		68×38	
E hot spot		11.35	07.3			3			
W hot spot		46 58.42	22.0			17			
0258+35A	4C35.06	02 58 44.72	35 38 39.9	14.0	0.0466	728		250	130
core						<10			
E lobe+tail						305		110×50	
W lobe+tail						416		123×79	
1130+33A	4C33.27	11 30 30.16	33 59 47.0	17.3		890		26	30
core		30.19	47.0			45	2.0×0.6 40		
N jet						59			
N lobe						514		15×15	
N hot spot		30.59	51.8			33			
S lobe						331		13×9	
S hot spot		29.87	35.3			35			
1151+38	4C38.32	11 51 17.46	38 28 30.0	17.3		936		80	85
core		17.40	30.0			29	0.4×0.3 110		
E lobe						493		39×25	
W lobe						410		37×22	
E hot spot		20.45	33.6			4			
W hot spot		14.47	24.3			7			
1151+29	4C29.44	11 51 37.95	29 32 50.4	19.0	0.3292	1537		22	152
core		37.97	50.1			25	< 0.2		
N lobe						927		9×12	
S lobe						575		14×5	
N hot spot		37.78	57.3			276			

Table 3. continued

B2 Name	Other Name	R.A. (1950) h m s	Dec. (1950) ° ′ ″	m vis	z	S mJy	Size FWHM P.A.	LAS arcsec	P.A. °
1529+35	3C320	15 29 29.70	35 43 48.5	18.0	0.3420	1770		18	80
core						<5			
E lobe						896		91×7	
W lobe						869		10×5	
1539+34	4C34.42	15 39 31.75	34 20 33.0	18.0	0.4018	791		63	27
core		31.81	34.0			10	0.4×0.3 46		
N lobe						347		31×14	
S lobe						440		22×13	
N hot spot		32.91	21 05.4			101			
S hot spot		30.71	20 09.9			82			
1547+30	4C30.29					1240		18	118
core		15 47 12.57	30 56 18.1			<14			
E lobe						367		7×6	
W lobe						854		10×7	
1707+34	4C34.45	17 07 49.31	34 29 36.0	15.5	0.0801	614		75	148
core						<10			
N lobe		49.15	43.4			300		22×35	
S lobe		49.96	24.4			316		49×50	
2244+36	4C36.47	22 44 12.81	36 40 41.5	16.3	0.0815	1990		12	37
core						<50			
N lobe						797		6×7	
S lobe						1196		6×6	
2249+37	4C37.66	22 49 06.34	37 57 45.3	15.2	0.0587	969		167	55
core		06.42	57 44.9			29	2.3×2.0 48		
core2		07.73	57 37.1			13	5.3×3.5 8		
halo						898		167×11	

Table 4. Observational data at 5 GHz

B2 Name	Other Name	R.A. (1950) h m s	Dec. (1950) ° ′ ″	S mJy	FWHM P.A. arcsec °	LAS arcsec	P.A. °
0136+39	4C39.04	01 36 33.66	39 41 52.6	191		377	63
core		33.58	51.6	12	1.5 ×<1.2 179		
E lobe				100		107×48	
W lobe				79		150×40	
0204+29	4C29.06	02 04 08.78	29 16 30.5	721		200	62
core		08.83	30.7	24	1.4 ×1.2 107		
E lobe				426		116×36	
E hot spot		16.81	17 28.5	131			
W lobe				250		73×41	
0258+35A	4C35.06	02 58 44.72	35 38 39.9	170		80	162
core				<4			
E lobe				55			
W lobe+tail				114			
1707+34	4C34.45	17 07 49.31	34 29 36.0	170		50	154
core		49.23	36.0	4			
N lobe				92			
S lobe				75			
2249+37	4C37.66	22 49 06.34	37 56 45.2				
core		06.42	57 45.1	17	<1.0		
core2		07.74	57 37.0	3	1.5 ×1.2 79		

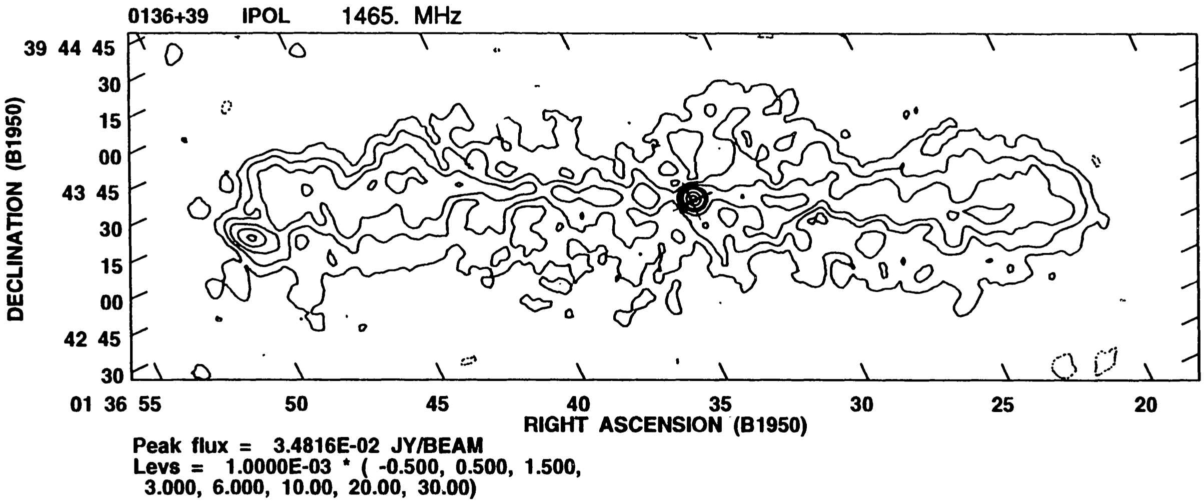

Fig. 1a.

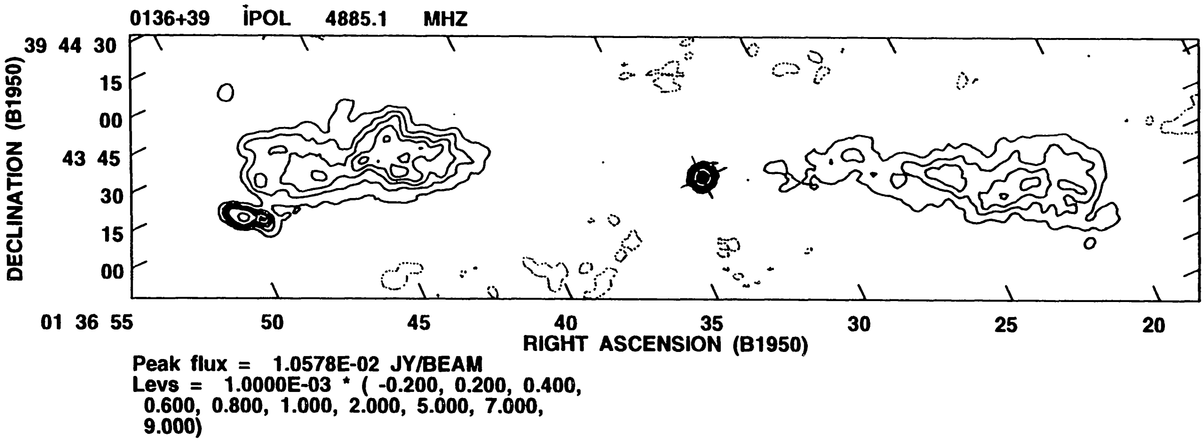

Fig. 1b.

Fig. 1-14. Contour maps. The source name is given at the top of the figures. The value of the contour levels is expressed in mJy/beam. The optical position is marked by a cross. Fig. a) shows the maps at 1.4 GHz data; Fig. b) shows the maps at 5 GHz data

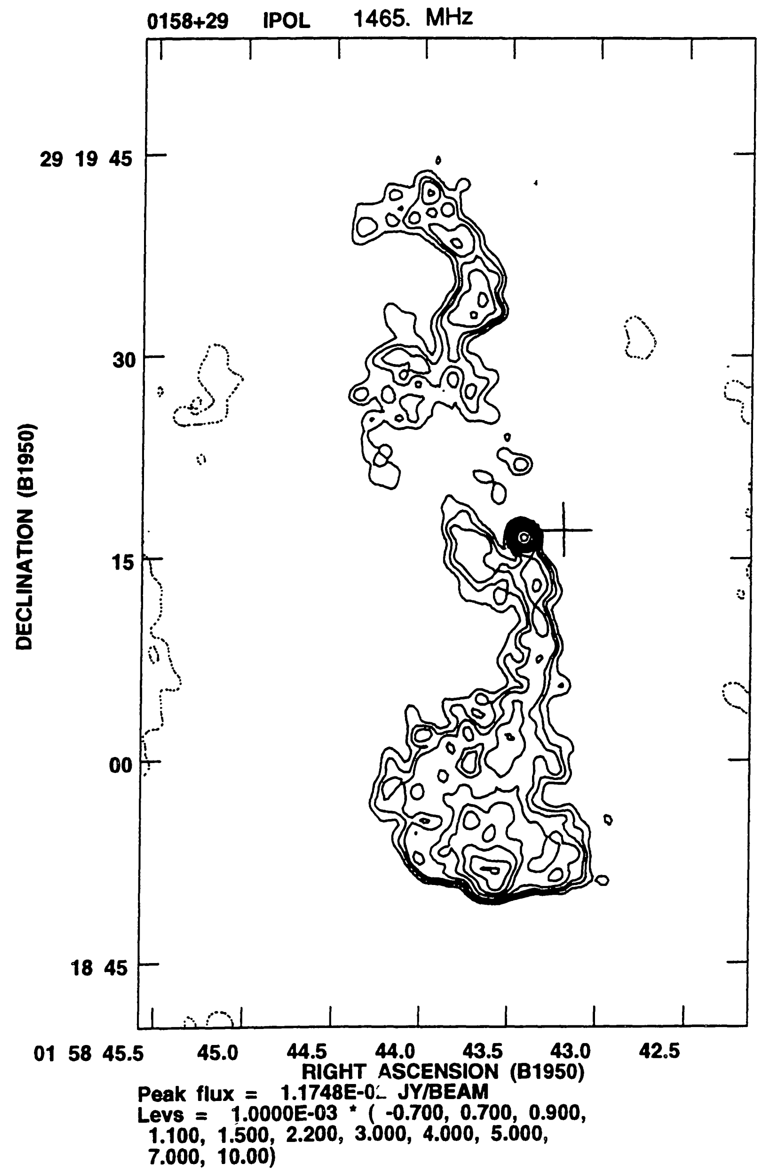
0158+29 IPOL 1465. MHz
29 19 45
30
15
00
18 45
DECLINATION (B1950)
01 58 45.5
45.0
44.5
44.0
43.5
43.0
42.5
RIGHT ASCENSION (B1950)
Peak flux = 1.1748E-0 JY/BEAM
Levs = 1.0000E-03 * (-0.700, 0.700, 0.900,
1.100, 1.500, 2.200, 3.000, 4.000, 5.000,
7.000, 10.00)

Fig. 2.

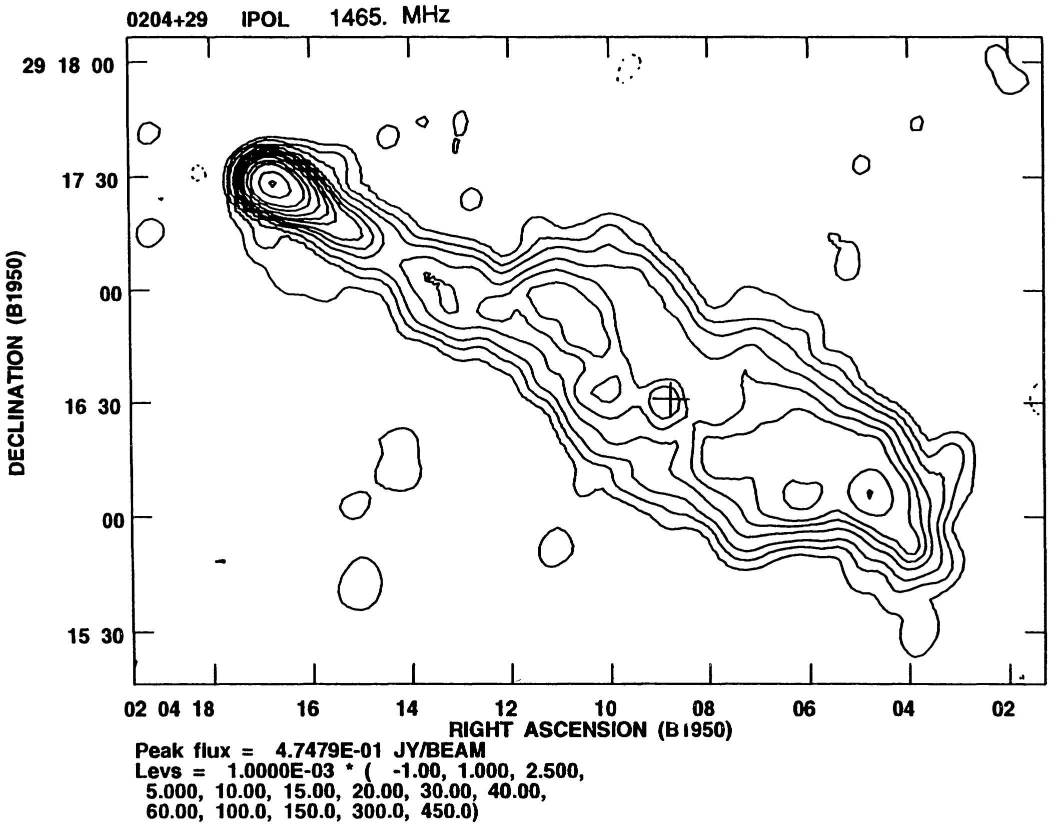
0204+29 IPOL 1465. MHz
29 18 00
17 30
00
16 30
00
15 30
DECLINATION (B1950)
02 04 18
16
14
12
10
08
06
04
02
RIGHT ASCENSION (B1950)
Peak flux = 4.7479E-01 JY/BEAM
Levs = 1.0000E-03 * (-1.00, 1.000, 2.500,
5.000, 10.00, 15.00, 20.00, 30.00, 40.00,
60.00, 100.0, 150.0, 300.0, 450.0)

Fig. 3a.

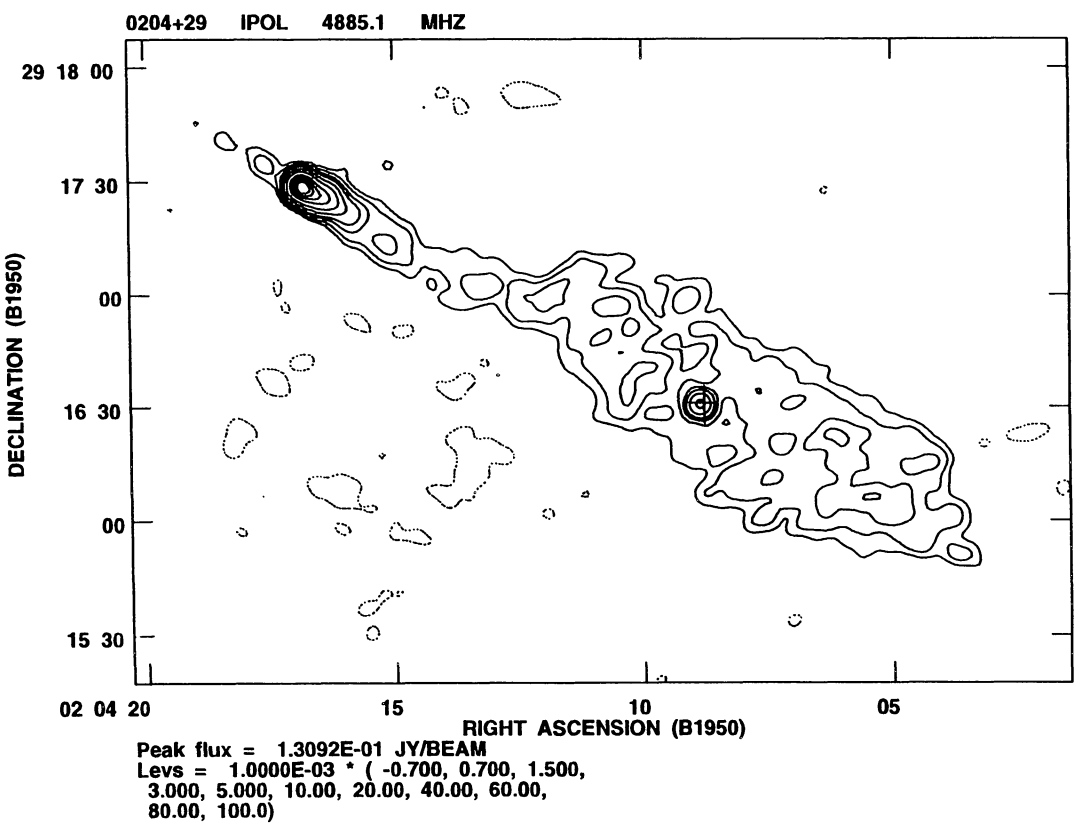
0204+29 IPOL 4885.1 MHZ
29 18 00
17 30
00
16 30
00
15 30
DECLINATION (B1950)
02 04 20
15
10
05
RIGHT ASCENSION (B1950)
Peak flux = 1.3092E-01 JY/BEAM
Levs = 1.0000E-03 * (-0.700, 0.700, 1.500,
3.000, 5.000, 10.00, 20.00, 40.00, 60.00,
80.00, 100.0)

Fig. 3b.

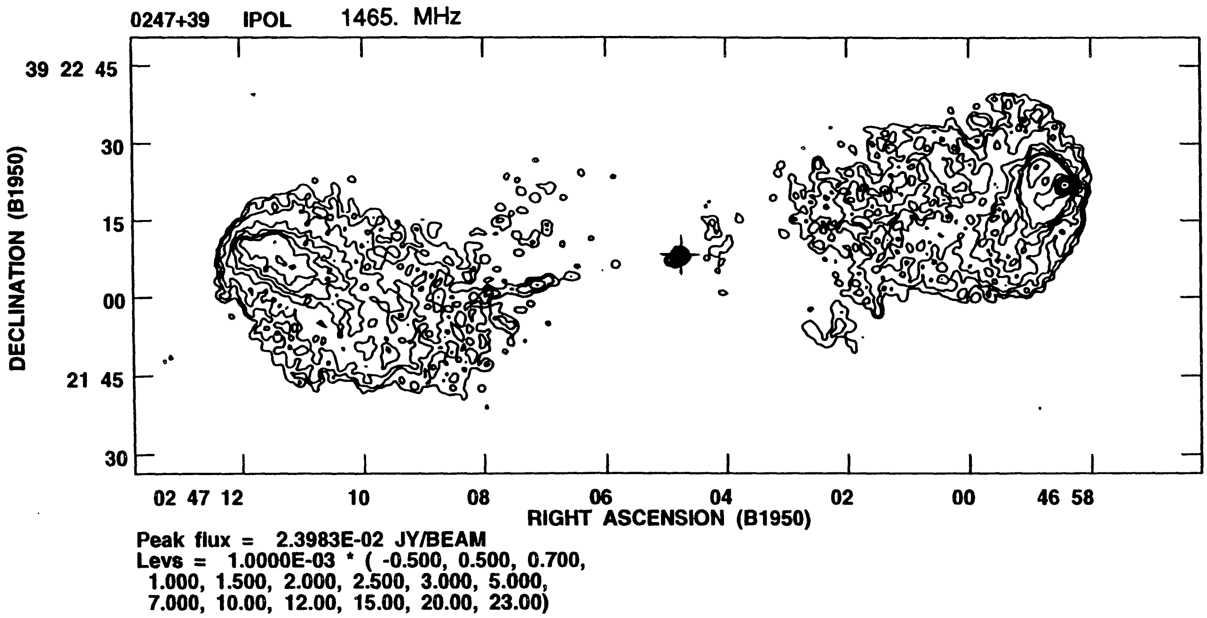
0247+39 IPOL 1465. MHz
DECLINATION (B1950)
39 22 45
30
15
00
21 45
30
02 47 12
10
08
06
04
02
00
46 58
RIGHT ASCENSION (B1950)
Peak flux = 2.3983E-02 JY/BEAM
Levs = 1.0000E-03 * (-0.500, 0.500, 0.700, 1.000, 1.500, 2.000, 2.500, 3.000, 5.000, 7.000, 10.00, 12.00, 15.00, 20.00, 23.00)

Fig. 4.

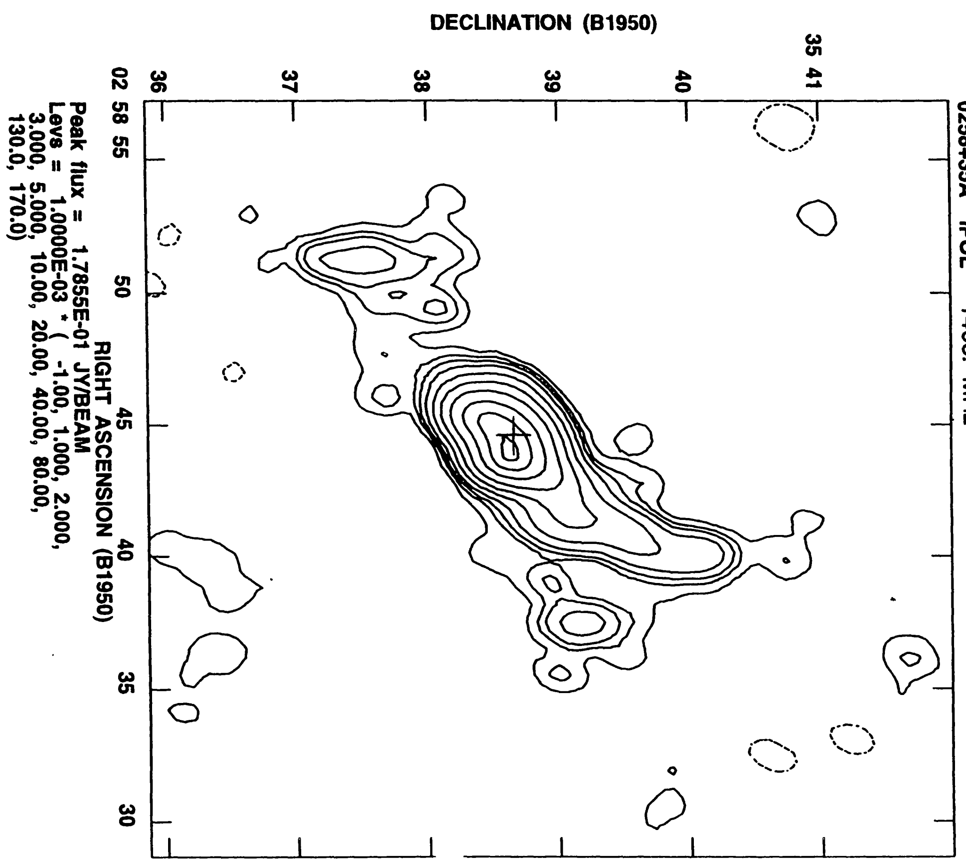
0258+35A IPOL 1465. MHz
DECLINATION (B1950)
35 41
40
39
38
37
36
RIGHT ASCENSION (B1950)
02 58 55
50
45
40
35
30
Peak flux = 1.7855E-01 JY/BEAM
Levs = 1.0000E-03 * (-1.00, 1.000, 2.000, 3.000, 5.000, 10.00, 20.00, 40.00, 80.00, 130.0, 170.0)

Fig. 5a.

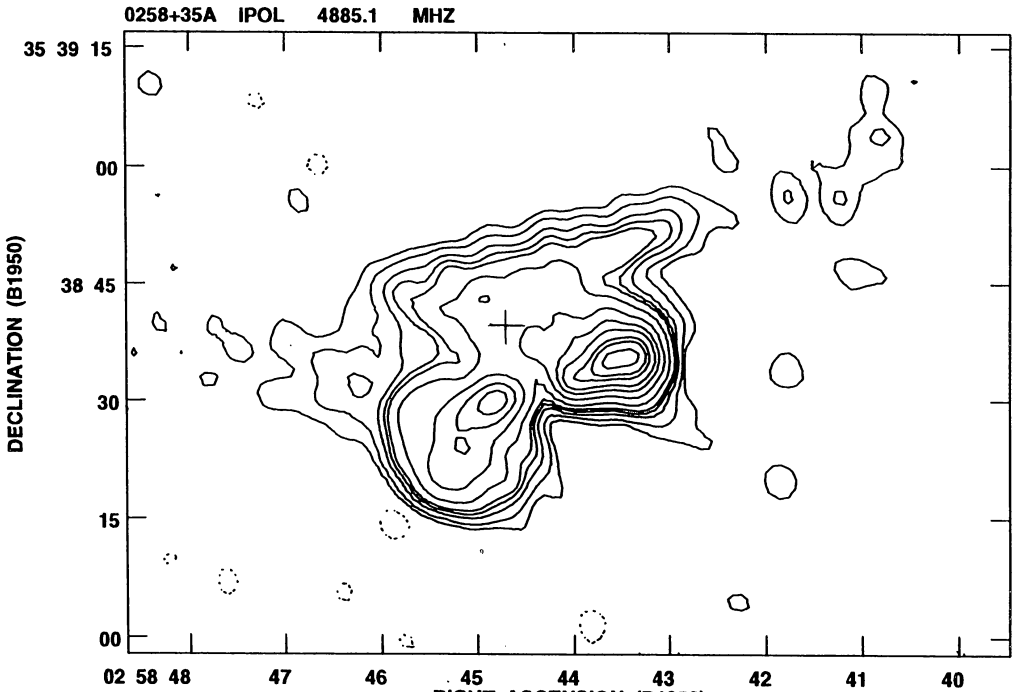

Peak flux = 1.6449E-02 JY/BEAM
Levs = 1.0000E-03 * (-0.100, 0.100, 0.200, 0.400, 0.600, 0.800, 1.500, 3.000, 5.000, 7.000, 10.00, 12.00, 15.00)

Fig. 5b.

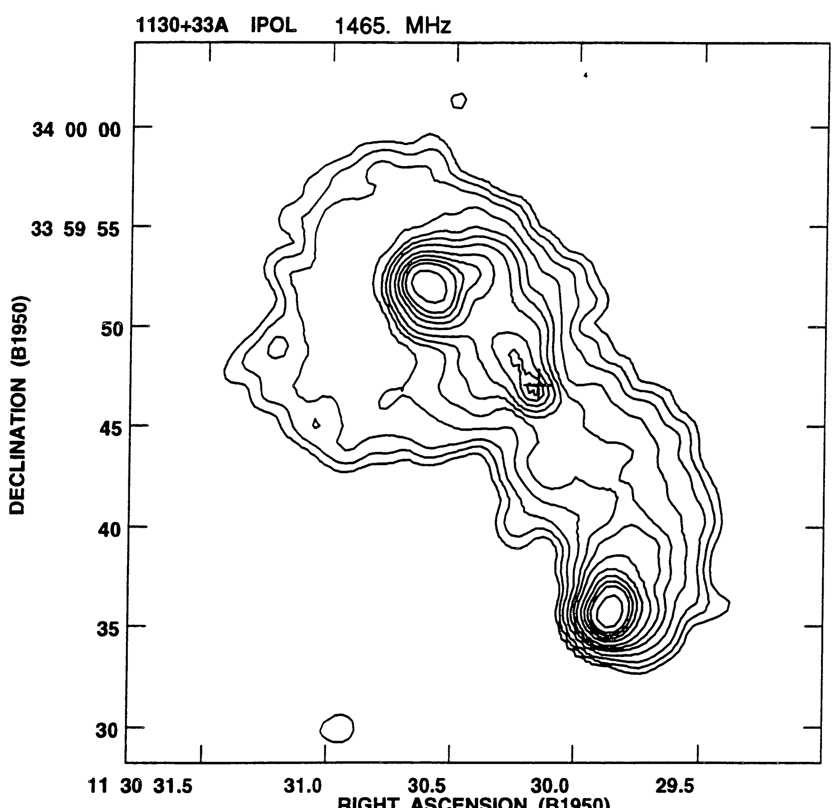

Peak flux = 5.1042E-02 JY/BEAM
Levs = 1.0000E-03 * (-0.400, 0.400, 0.800, 1.500, 3.000, 5.000, 7.000, 10.00, 15.00, 20.00, 25.00, 30.00, 40.00)

Fig. 6.

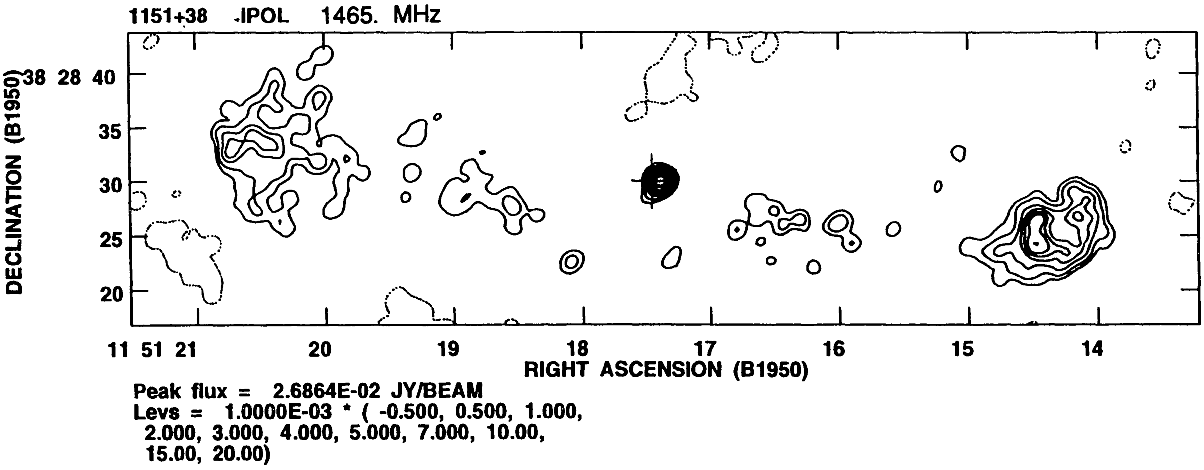
1151+38 IPOL 1465. MHz
38 28 40
35
30
25
20
DECLINATION (B1950)
11 51 21
20
19
18
17
16
15
14
RIGHT ASCENSION (B1950)
Peak flux = 2.6864E-02 JY/BEAM
Levs = 1.0000E-03 * (-0.500, 0.500, 1.000, 2.000, 3.000, 4.000, 5.000, 7.000, 10.00, 15.00, 20.00)

Fig. 7.

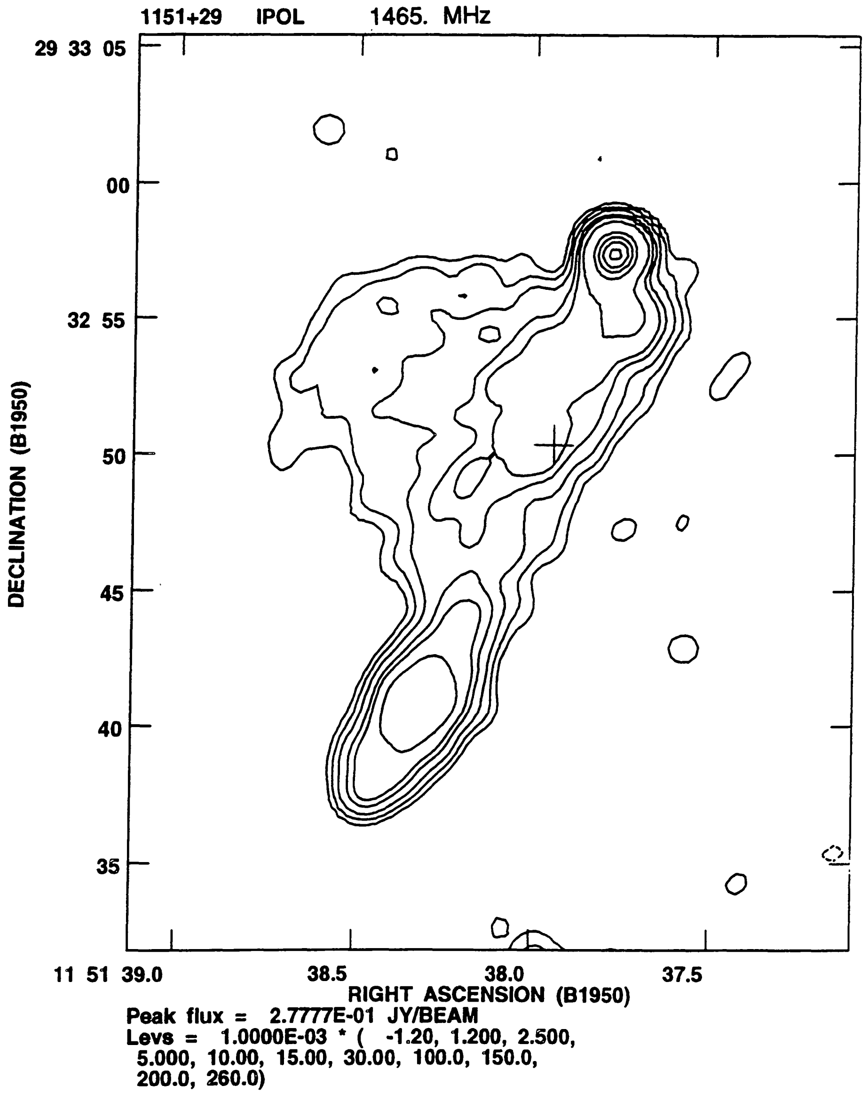
1151+29 IPOL 1465. MHz
29 33 05
00
32 55
50
45
40
35
DECLINATION (B1950)
11 51 39.0
38.5
38.0
37.5
RIGHT ASCENSION (B1950)
Peak flux = 2.7777E-01 JY/BEAM
Levs = 1.0000E-03 * (-1.20, 1.200, 2.500, 5.000, 10.00, 15.00, 30.00, 100.0, 150.0, 200.0, 260.0)

Fig. 8.

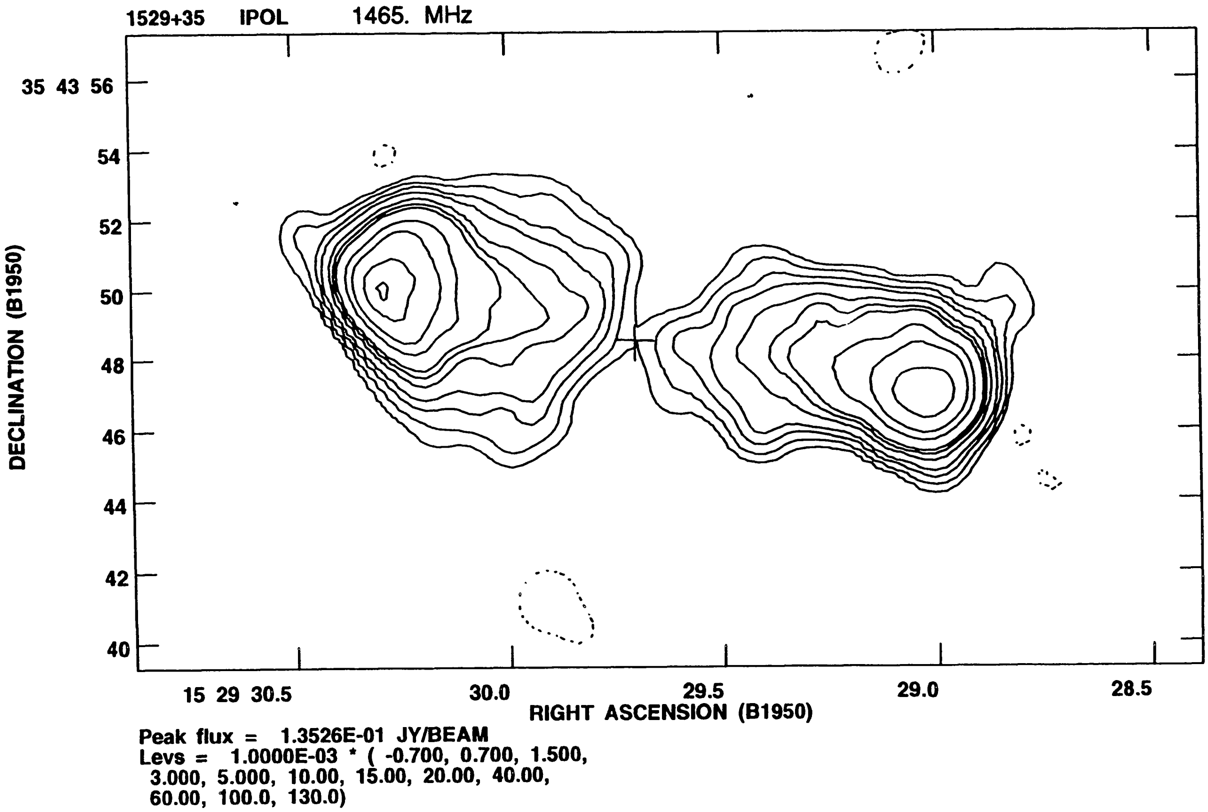
1529+35 IPOL 1465. MHz
35 43 56
54
52
50
48
46
44
42
40
DECLINATION (B1950)
15 29 30.5
30.0
29.5
29.0
28.5
RIGHT ASCENSION (B1950)
Peak flux = 1.3526E-01 JY/BEAM
Levs = 1.0000E-03 * (-0.700, 0.700, 1.500, 3.000, 5.000, 10.00, 15.00, 20.00, 40.00, 60.00, 100.0, 130.0)

Fig. 9.

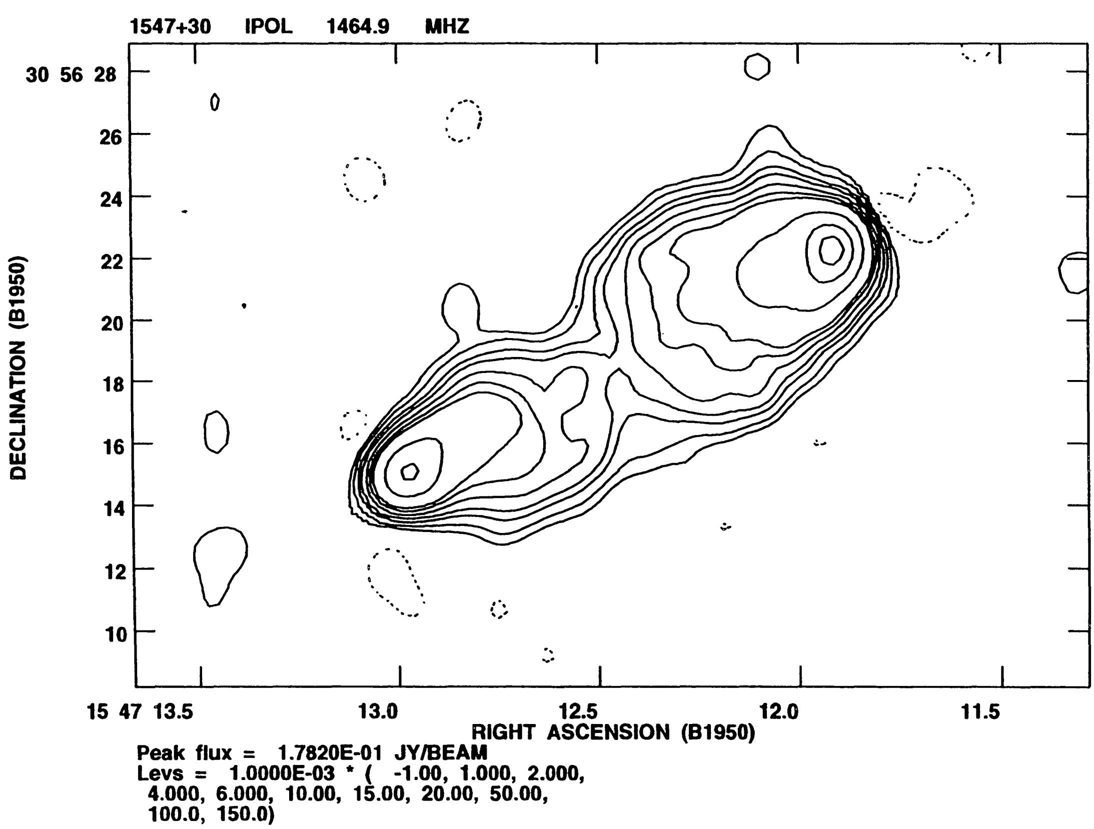
1547+30 IPOL 1464.9 MHZ
30 56 28
26
24
22
20
18
16
14
12
10
DECLINATION (B1950)
15 47 13.5
13.0
12.5
12.0
11.5
RIGHT ASCENSION (B1950)
Peak flux = 1.7820E-01 JY/BEAM
Levs = 1.0000E-03 * (-1.00, 1.000, 2.000, 4.000, 6.000, 10.00, 15.00, 20.00, 50.00, 100.0, 150.0)

Fig. 11.

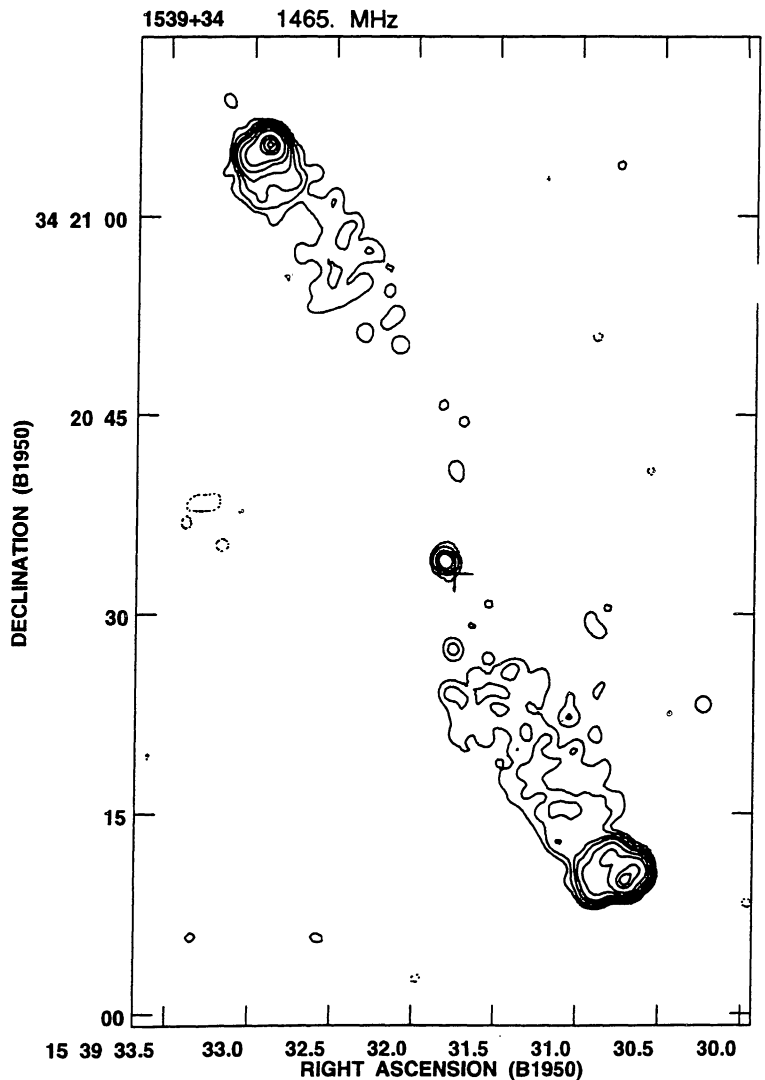

Peak flux = 1.0143E-01 JY/BEAM
Levs = 1.0000E-03 * (-0.700, 0.700, 1.500, 3.000, 5.000, 10.00, 20.00, 50.00, 70.00, 90.00)

Fig. 10.

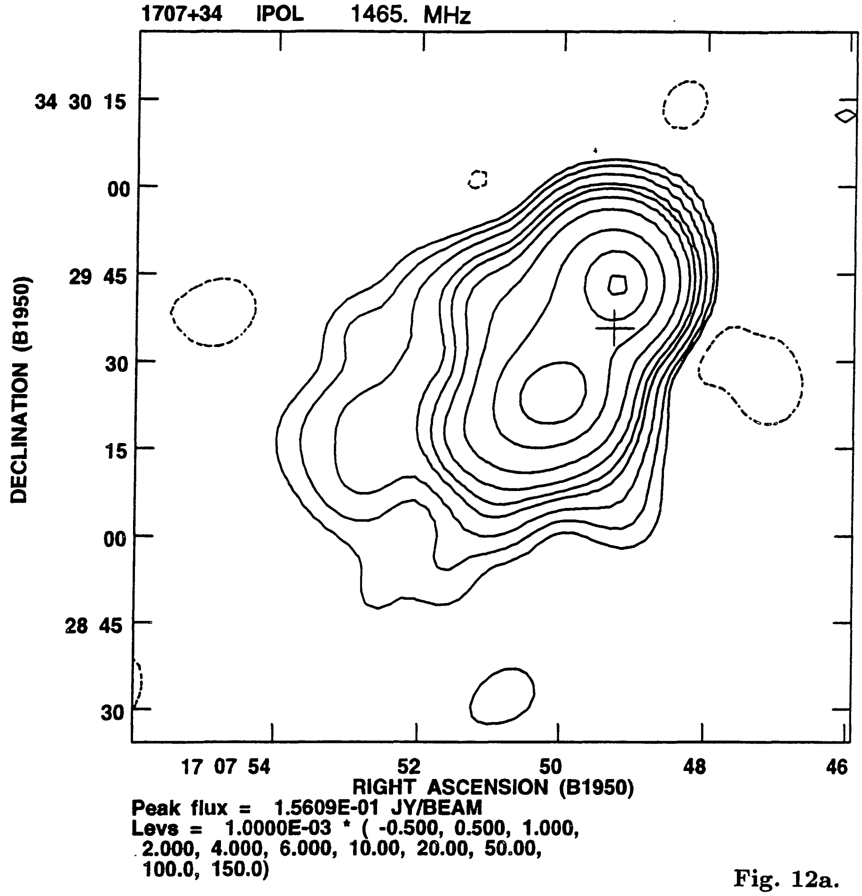

Fig. 12a.

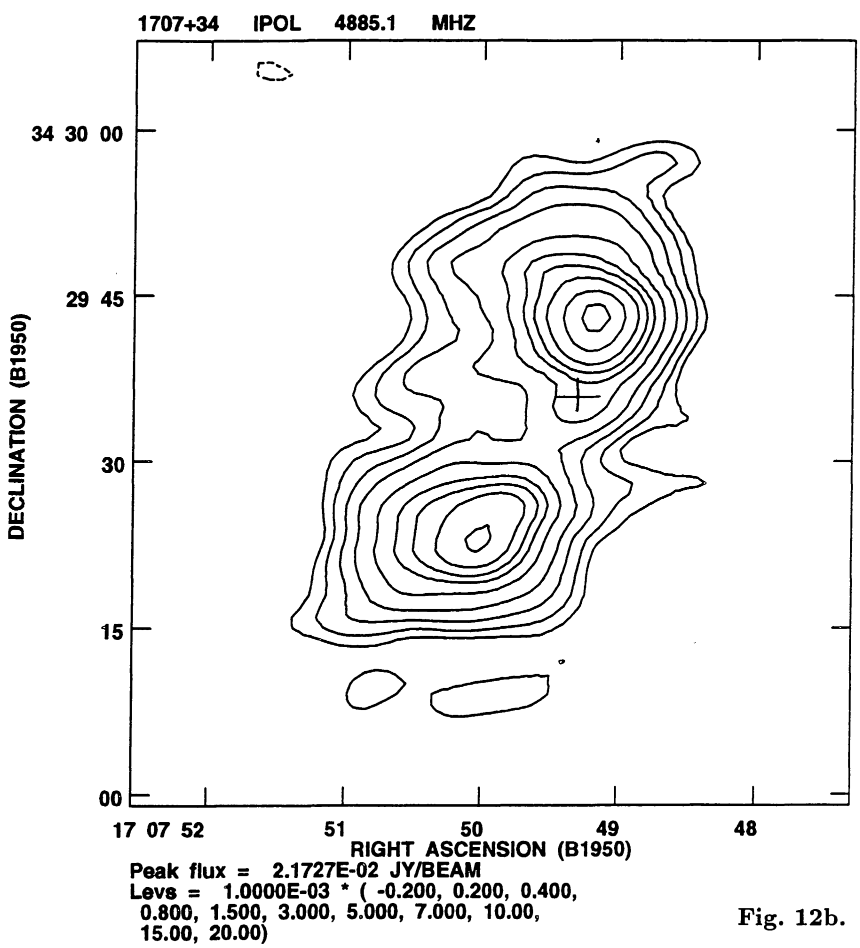

Fig. 12b.

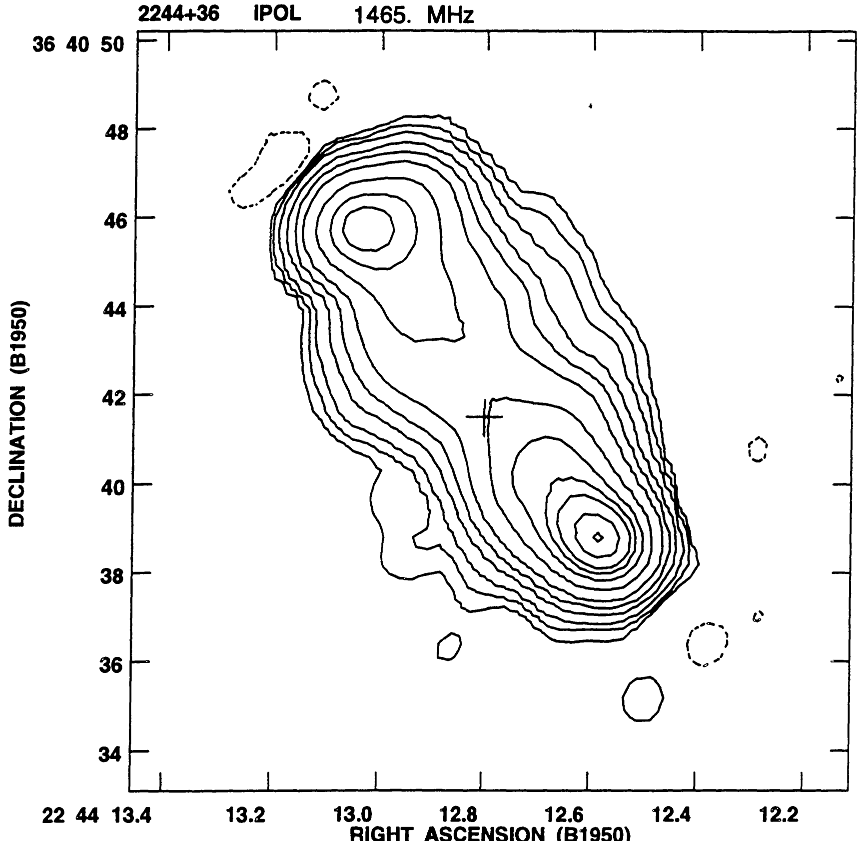

Peak flux = 4.1727E-01 JY/BEAM
Levs = 1.0000E-03 * (-0.500, 0.500, 1.000, 2.000, 5.000, 10.00, 20.00, 50.00, 100.0, 150.0, 200.0, 300.0, 400.0)

Fig. 13.

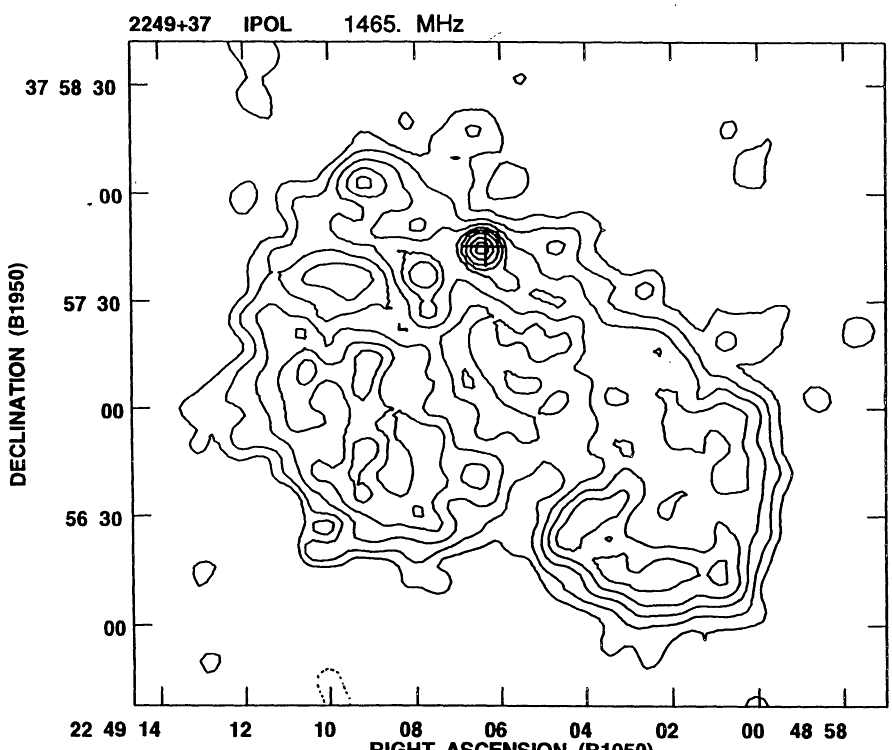

Peak flux = 2.2248E-02 JY/BEAM
Levs = 1.0000E-03 * (-0.700, 0.700, 1.500, 3.000, 5.000, 7.000, 10.00, 15.00, 20.00)

Fig. 14.